

Fluka simulations for the Neutron Generator test at the Vertical Drift cold box

This notes describes a standalone FLUKA[?, ?, ?] simulation of the test performed with the CERN Vertical Drift Coldbox and an external neutron generator in spring 2024. It is also intended as a reference for the use of the simulated ntuples. Descriptions of the D-D generator and of the experimental setup are in [?, ?]. There is no attempt here of a detailed analysis of the simulations and/or comparison with data. Nonetheless, a few results are shown and preliminary deductions are put forward. Namely, the predominant effect of external material in the neutron capture process is highlighted.

1 Geometry

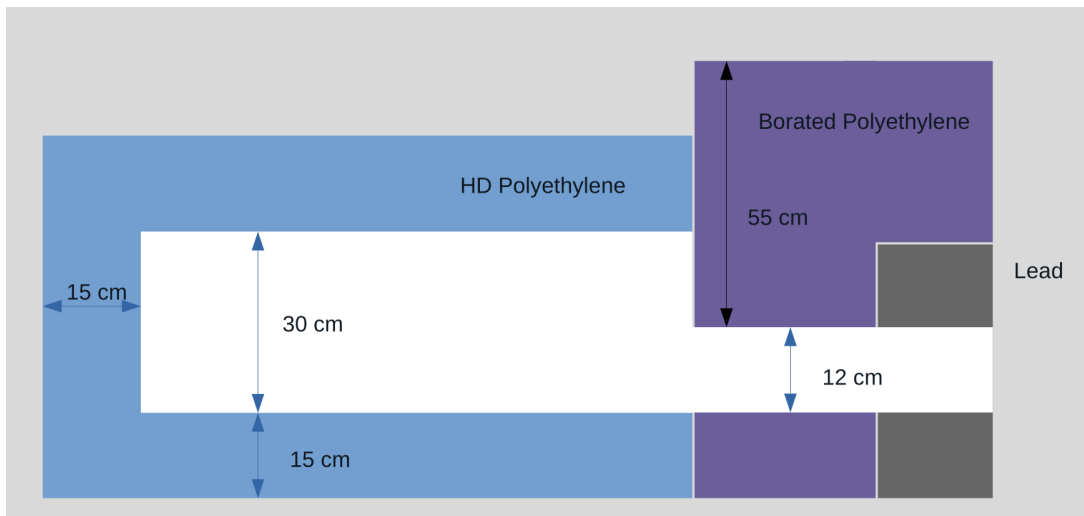


Figure 1: Cross section of the neutron generator shielding, courtesy of Walker Johnson

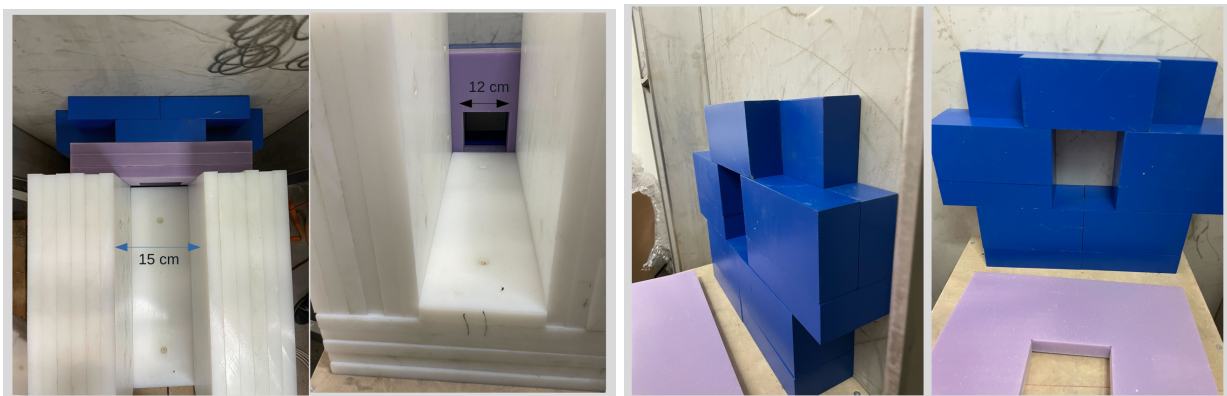


Figure 2: Photos of the neutron generator shielding. Lead Blocks used are 5cm x 10cm x 20cm. courtesy of Walker Johnson

The simulation setup includes the cryostat, the Photon Detector System (PDS), the neutron generator and its shielding, the anode and its supporting structure. In the following, the Liquid Argon region contained in the volume defined by the anode transverse dimensions, the first anode vertical position and the cathode position is referred to as *Active LAr*.

Dimensions and densities of the various parts are:

- Cryostat inner membrane : Fe7Cr2Ni steel thickness 0.12cm $\rho = 7.93g/cm^3$

- Cryostat insulation: polyurethane foam, $C_{17}H_{16}N_2O_4$, $\rho = 0.035g/cm^3$, 40cm in each dimension
- Cryostat external Steel support: Fe7Cr2Ni 1 cm thick
- 4 PD modules, 60x60 cm, 0.5cm thickness, assumed plastic
- PDS frame G10, 2.5 cm lateral 1.5 cm thick
- Drift distance 22.6 cm as derived by data
- Inner membrane dimension 100 x 389 x 391.3 cm
- Active LAr transverse dimensions 337 x 299.3 cm
- Ar gas starting 60 cm from the bottom of the active LAr
- Two anode planes, G10, 0.32 cm each, separated by 1 cm. Density is one half of G10 one to account for holes.
- plastic support of the anodes: epoxy-glass, total thickness 6.5 cm, density adjusted to match the actual weight of 35 kg
- steel support of the anode planes mimicked with three thick bars (S6x12.5) and three thin bars (S4x7.7) with density adjusted to match the linear weights (18.6 kg/m and 11.5 kg/m)
- The neutron generator shielding as in figures 1, 2
- Borated polyethylene has 5% Boron in weight
- Tube of the neutron generator: 55 cm length, 11 cm diameter, 0.25 cmthickless, steel. This is a wild guess: only the external dimensions are known, both of the tube and of the electronic box. The density has been adjusted in order to match a total weight (tube + box)of 12 kg as in the datasheet.

A cross section of the geometry is in figure 3.

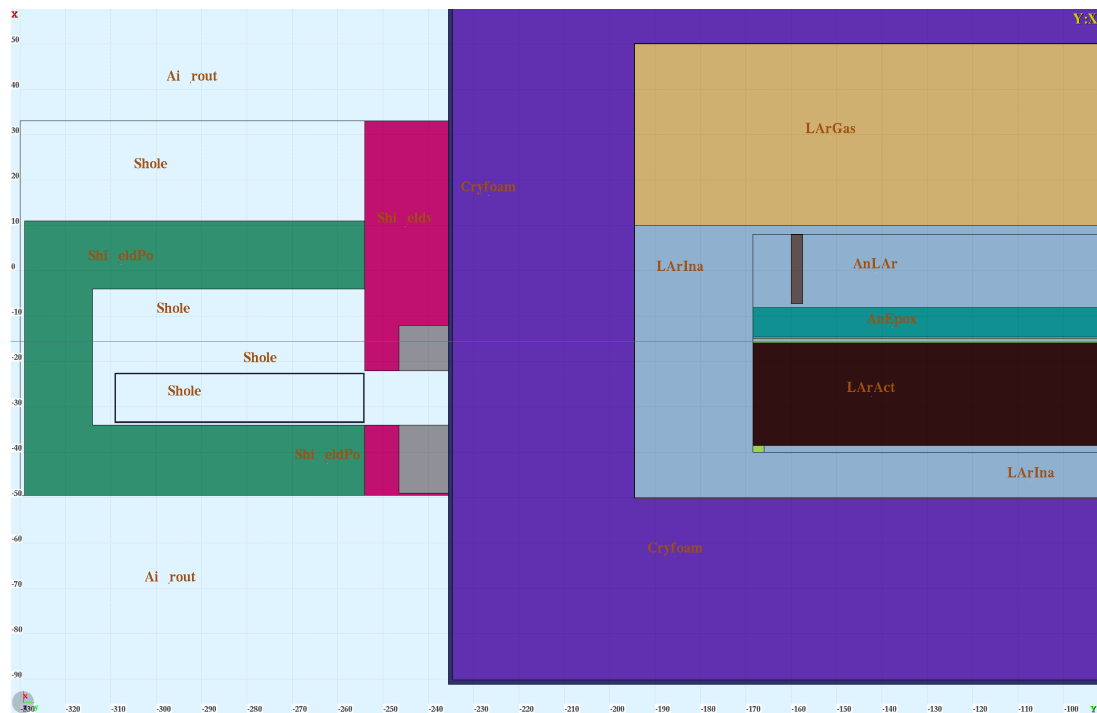


Figure 3: y-x cross section of the geometry

The coordinate system has the x axis in the vertical direction, the z axis in the “Salève-Jura” direction. Origin of coordinates is the centre of active volume in y and z. Instead, in the drift direction the active LAr is in the negative

space, between -38.5 cm and -17.5 cm. The photon detectors tiles and the neutron generator are positioned as in figure 4. The neutron generator is displaced horizontally by 60 cm with respect to the center of the active volume, while it is centered in the vertical direction.

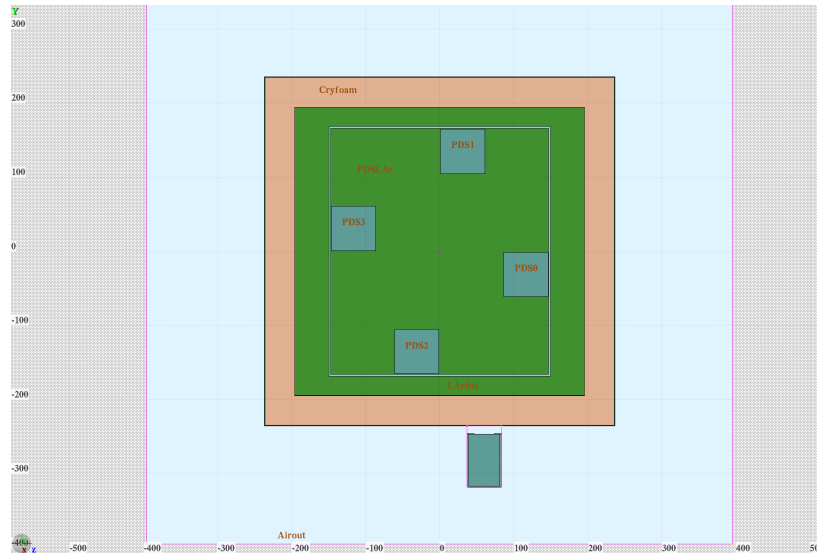


Figure 4: positions of the PDS tiles and of the neutron generator. In this plot, z axis is horizontal, y axis vertical. (x-axis is drift direction)

2 Tracking and scoring

Monochromatic neutrons with kinetic energy equal to 2.5 MeV are emitted isotropically from a point situated at the centre of the hole in the neutron generator shielding, at a distance of 14 cm from the end of the neutron generator tube, equivalent to 31.5 cm from the external cryostat structure. The possibility, available in FLUKA, to generate neutrons according to a realistic D-D spectrum and angular distribution has not been exploited because of the uncertainty on the operating voltage of the generator.

All neutrons are emitted at time=0.

Neutron transport and interactions are simulated with the new point-wise correlated algorithm of FLUKA.

All products from neutron interactions in all parts of the geometry are generated and tracked.

Optical photons are produced and transported in the LAr regions, both in the readout volume (“active LAr”) and the one around it or above the anodes (“inactive LAr”) The optical photon intensity is $2.4 \cdot 10^4$ optical photons/MeV. This corresponds to emission at an electric field of 500V/cm.

Given a PDS efficiency of 3%, one photoelectron corresponds to ≈ 33 optical photons, thus an energy deposition of at least 2.8 keV (if immediately above a tile, considering half of the solid angle)

Production has the two Ar time constants. Transport has Rayleigh length=90cm. In order to decrease CPU time, only 1/10 of the optical photons are tracked.

Only events where there is either energy deposition in active LAr, or one neutron capture in active LAr, or photoelectrons arriving at the tiles are recorded.

Recorded events correspond to about 1.5% of generated neutrons.

Events with one neutron capture are about 0.04% of the generated neutrons

The word “about” reflects a strong dependence of these numbers from the material composition of the setup. For instance, changing the composition of the neutron generator shielding from HDPE ($\rho = 0.96 \text{ g/cm}^3$, $(\text{C}_2\text{-H}_4)_n$) to Polystyrene ($\rho = 1.06 \text{ g/cm}^3$, $(\text{C-H})_n$) increases the fraction of recorded events to 2% and the capture ratio to 0.07%.

2.1 recorded quantities

2.2 Optical photons: time structure

The Units used are:

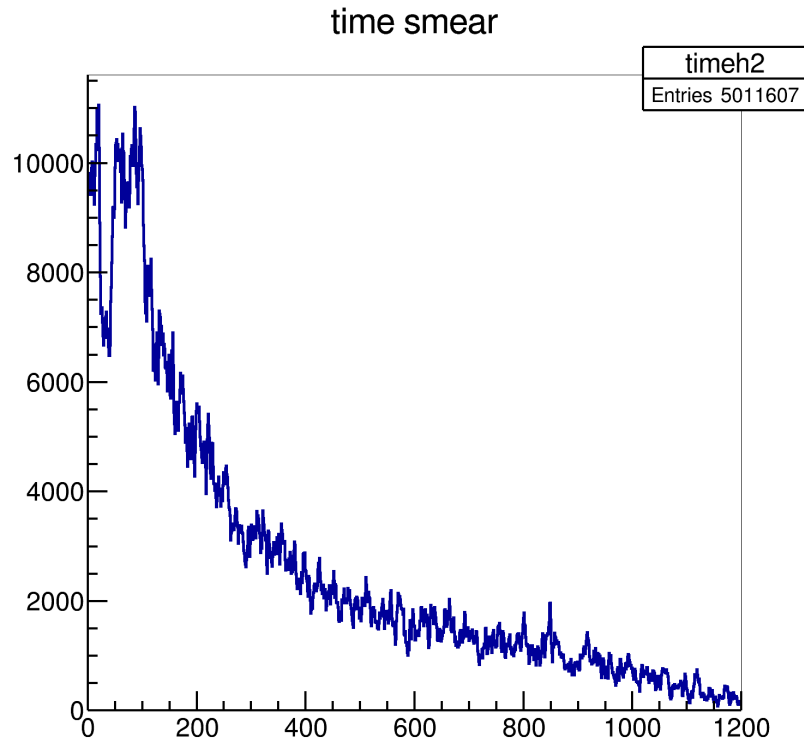


Figure 5: number of hits as a function of time after trigger in microseconds. After randomization of neutron start time

- Energies and momenta: GeV (or GeV/c)
- Lengths: centimeters
- Time: nanoseconds

Each event corresponds to one neutron from the neutron gun

The output is in form of root Trees.

They record interactions occurring in all regions and contain energy depositions and optical photons.

- Inelastic interactions: they are recorded if they produce at least
 - One electron or one photon above 100 KeV
 - Or one charged hadron
 - or one light nucleus (up to α) above transport threshold
- “Boundary Crossing” : particle entering/exiting the various regions
- “Stopping” : particles going below transport threshold, except residual nuclei.

Particle types, energies, type of interaction, positions and times are recorded.

In addition, the n-tuple contains energy deposits in the active LAr and optical photons arriving at the detectors, without distinguishing the particle that originated them. No time information is available for energy depositions. More correlated information can be provided in the future if deemed necessary.

- Energy deposited in the active LAr, divided in cells with dimensions approx 1x2x2cm
- The same, counting only depositions from neutron captures occurred in the active LAr

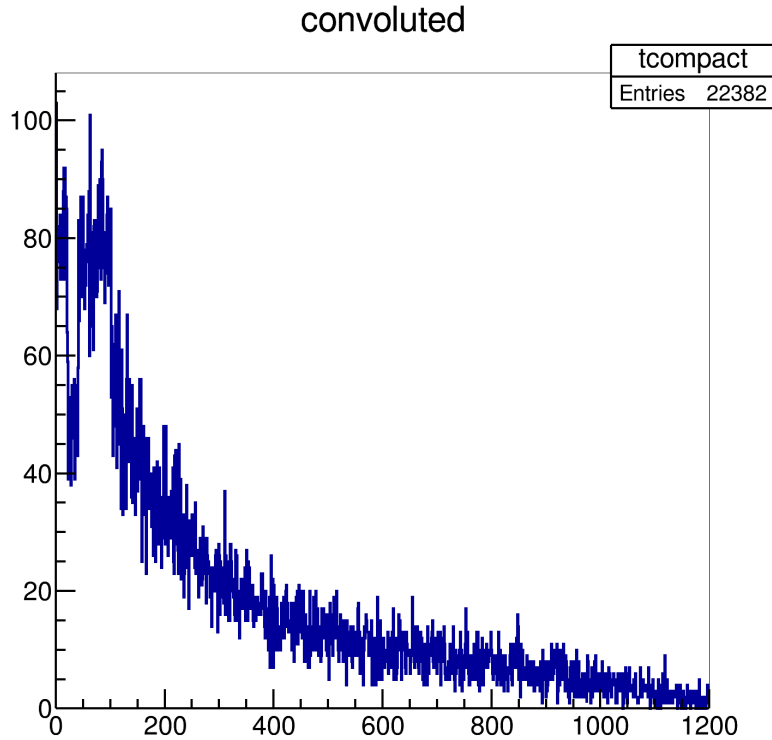


Figure 6: number of hits as a function of time after trigger in microseconds, after randomization of neutron start time, convolution with single phe response and peak finding

- Number of optical photons arriving at each photon detector in intervals of 16 nanoseconds, within 1.2 milliseconds. *divided by ten*
- The same, counting only optical photons from neutron captures in the active LAr
- total energy deposited in the active LAr
- total number of optical photons in each photon detector summed over time *divided by ten*
- total number of optical photons summed over time and photon detectors *divided by ten*

The detailed list of the n-tuple variables is in the Appendix.

3 Analysis and results

All figures presented below have been obtained by simulating 2×10^7 neutrons from the neutron generator. No attempt has been made at any normalization, all plots are in arbitrary units. In order to compare with the experimental distribution of optical photons detection times, it is necessary to reproduce offline the bunched structure of the neutron generator pulse.

For each event, a random time is assigned to the original neutron, assuming a time structure with 5 bunches, each one $60 \mu\text{sec}$ separated by 20 nanoseconds, of which only the last one and a half are in the trigger window.

We concentrated for the moment on the Photon Dectector tile nearest to the neutron generator. For all events in which the total number of photoelectrons in this tile is larger than a threshold set equal to 10, the arrival times of optical photons have been histogrammed after neutron time randomization. The conversion from optical photons to photoelectrons is made assuming an efficiency of 3%. The result is shown in figure 5, in qualitative agreement with experimental data (the latter after subtraction of a constant pedestal due to cosmic rays)

Figure 5 is not fully representative of real data, since the shaping and integration from the electronics chain is missing. Often, there are many small signals very close in time that would be integrated together by the electronics,

thus changing the number of signals, and maybe reaching the readout threshold when the single ones didn't. However, this simplistic approach does get back the same shape as in data.

Indeed Monte Carlo simulations should be convoluted with the response of the electronics and treated with the same peak finding algorithm as real data.

To this aim, a first attempt has been done to convolute the optical photons with the response of the electronics, and try to find the peaks above threshold, as in figure 6. The result is similar to the one in 5, except of course the normalisation. No further work has been done in this direction yet.

Figure 5, as well as data, shows a clear accumulation of signals at very short times from the neutron production, followed by an exponentially decreasing tail and possibly an almost constant pedestal visible at the very end of the time frame. These three components can be well identified in the simulation.

Considering only the most active tile, and only events with at least 10 total photoelectron, the response can be separated in different event classes, namely

- events in which a neutron capture occurred inside the active LAr
- events in which a neutron inelastic interaction occurred in the active LAr (due to the low neutron energy those are inelastic scattering with production of one photon)
- events where there was no neutron interaction in the active LAr, rather the scintillation light was produced by electrons or gammas generated by neutrons in the surrounding materials.

Time response from the three event classes, after time randomization as described above, is shown in figure 7. This plot clearly shows that capture events are a minority and produce an almost flat signal distribution. Inelastic interactions in LAr are centered around the neutron production time, while the exponential tail is essentially due to neutron events external to the active LAr.

This is an annoying conclusion, since it appears to prevent the use of this test beam for studying the time evolution of neutron propagation in LAr.

The region where the neutrons originate those “background” signals are graphically depicted in figure 8. The largest contribution comes from the polyethylene shielding of the neutron generator, followed by the outer steel layer of the cryostat and by the inactive LAr region. There is a contribution from the neutron gun tube, that is at this moment questionable, but does not influence the overall understanding.

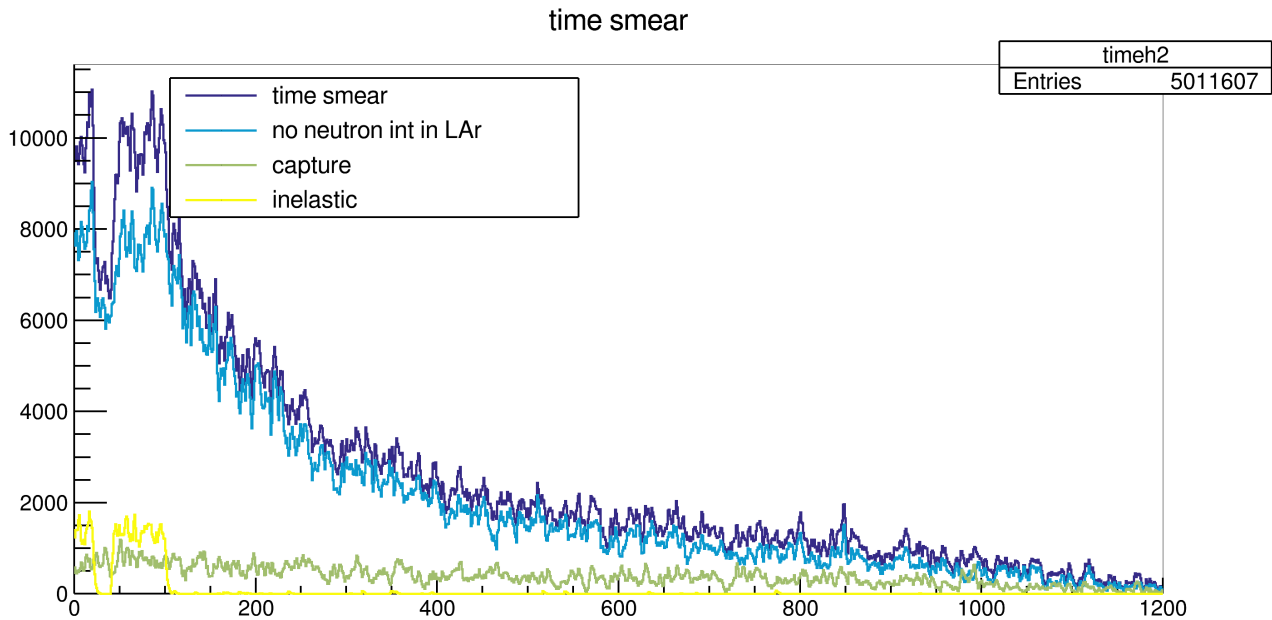


Figure 7: Time distribution of optical photons (in microseconds) from all events (dark blue), from events with a neutron capture in active LAr (green), from events with inelastic neutron interactions in active LAr (yellow) and from events with no neutron interaction in active LAr (light blue)

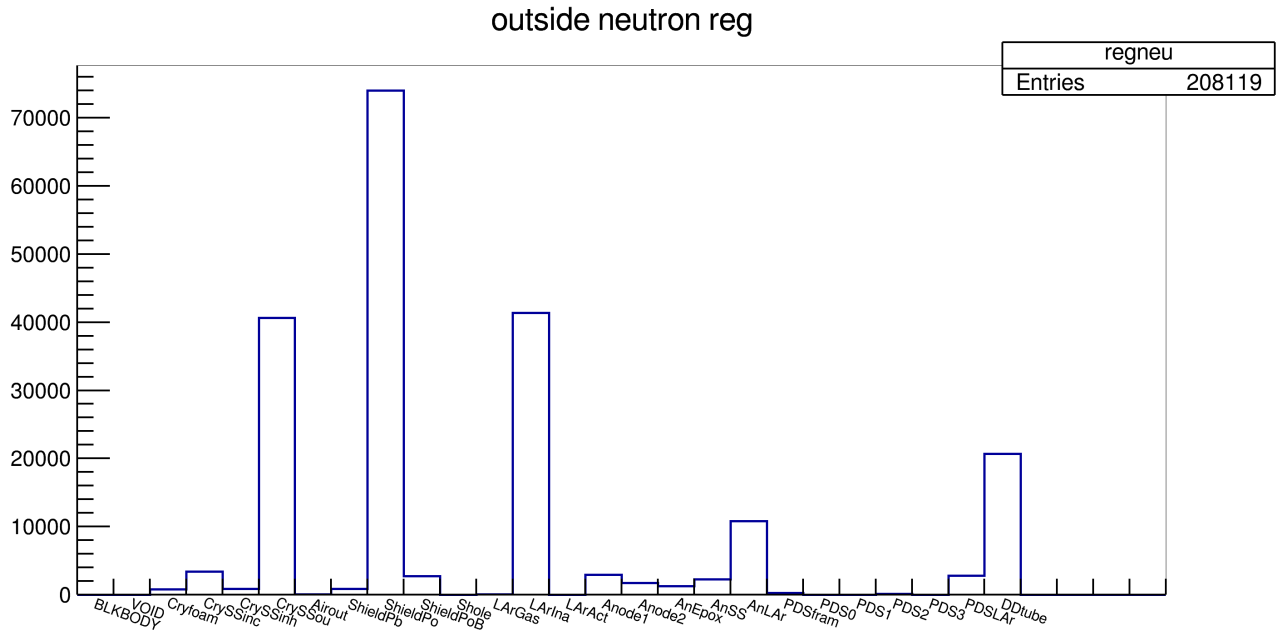


Figure 8: non-active regions where neutron interactions occur (from the NeuRegSec variable) finally producing a charge signal in the active LAr and a number of photoelectrons above threshold in the most active tile.

4 Total deposited energy

Figure 9 shows three spectra of the total deposited energy in the LAr active volume, obtained by summing up the deposits in all calorimetric cells.

No threshold has been set on the energy deposition in single cells (a cell is 1x2x2 cm wide). Note the logarithmic scale, necessary to visualize the high energy part.

The dark blue curve includes all events. It extends above the energy released by neutron capture on ^{40}Ar (6.1 MeV), due to energetic γ s from steel.

The green-ish curve is energy deposited in events with a neutron capture in the active Ar. The tail above 6.1 MeV is due to capture on other Ar isotopes.

The yellow curve is obtained from capture events by summing only cells flagged as filled by products of the neutron capture. It is almost indistinguishable from the green one, showing that neutron capture events are clean from background. This does not mean that there can be clean events, both because of other external and internal backgrounds, and because a single spill of the neutron generator contains many neutrons. How many is not known, especially because the generator was operated in external trigger mode. Just to get an idea, in standard operation it delivers 10^6 neutrons/second at 250Hz, thus 4000 neutrons/spill. This would imply 60 “visible” events per spill on average, of which 1.6 would neutron capture in the active LAr.

5 Photon spectra

The new point-wise correlated neutron transport of FLUKA provides a simulation of photon spectra after inelastic interactions, including capture, that is based on known nuclear energy levels and branching ratios, supplemented by a statistical deexcitation model.

The spectrum of capture γ -rays from Argon is shown in figure 10. Contributions from Ar isotopes different from ^{40}Ar is visible, since the material is simulated in its natural isotopic composition.

The spectrum of γ -rays from inelastic and capture in all other materials present in the geometry is shown in figure 11. The 2.2 MeV γ from capture on hydrogen is well visible, as well as the 7.6 MeV γ from capture on Iron.

Both spectra are constructed from γ rays as they are generated, without any requirement on signal thresholds.

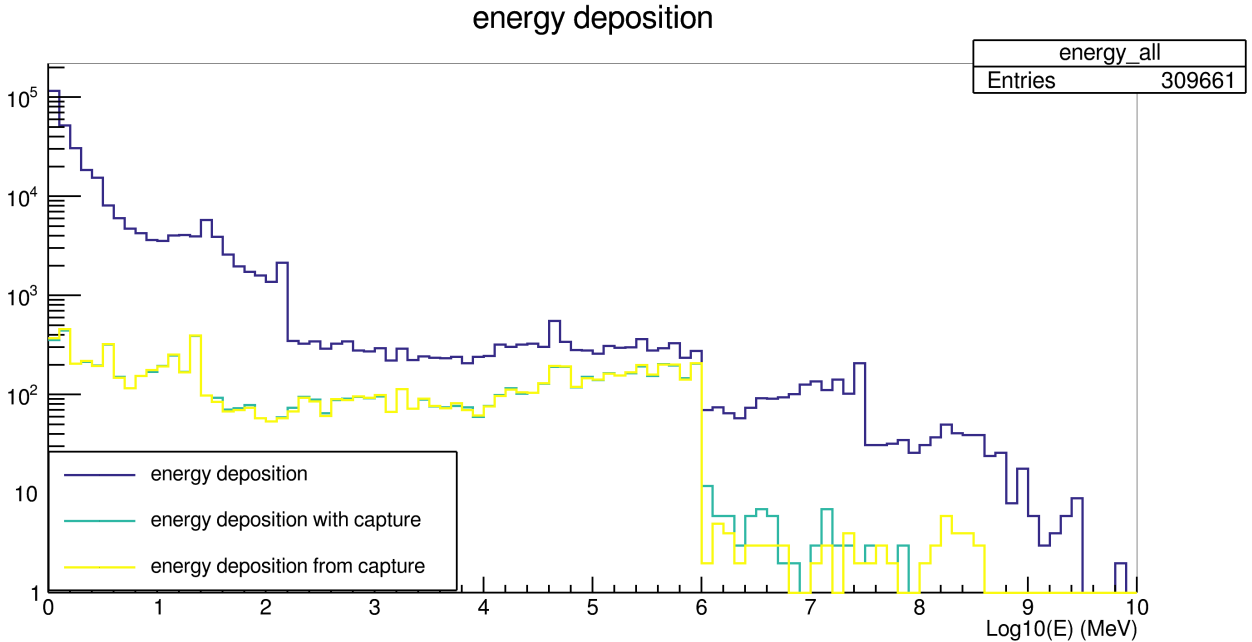


Figure 9: energy spectra from all events, from events with a neutron capture in the active LAr, and strictly from neutron captures

6 Neutron histories

The analysis of neutron “histories” allows to further understand the roles of the various parts of the experimental setup in building the signal.

In particular, it is important to understand whether the neutron moderation occurs in Argon or elsewhere.

To this aim, events with a neutron capture in the active LAr region have been selected. For each of them, the neutron path has been backtraced and three energy spectra have been constructed:

1. The energy of the neutron when it first exits from the inner membrane of the cryostat
2. The energy of the neutron at the last time that it exits from the inner membrane of the cryostat, meaning that it re-entered the walls and scattered back before being captured
3. The energy of the neutron when it enters the active volume before being captured

Those three spectra are drawn in figure 12. It can be seen that most of the neutron captured in the active LAr have been already moderated before passing the inner membrane, they can be further moderated by rescattering, both in the cryostat again or in the materials surrounding the active volume.

7 Particle-level energy clusters

It has been pointed out that a good signal of the presence of neutron capture could be the detection of the 4.7 MeV deexcitation γ . A first step in its identification could be the detection of a single energy cluster corresponding to the energy deposited by the e^+e^- after pair production. Assuming that the two annihilation γ s will convert further away, The energy of this cluster will correspond to the so-called double escape peak.

A first assesment of the possibility to perfor such a measurement can be attempted at particle level, without the need of a full reconstruction.

Since all energy depositions are finally due to electrons/positrons, it can be assumed that every time an electron is generated, a corresponding energy cluster is deposited. The spectrum of energy clusters can be obtained by inspecting all secondary interaction vertexes in the active LAr region. To avoid double counting, only interactions initiated by γ are considered, not those initiated by electrons. A small double counting could still exist due to bremsstrahlung, however it should be small given the low energy range. All electron/positron energies from the same interaction are

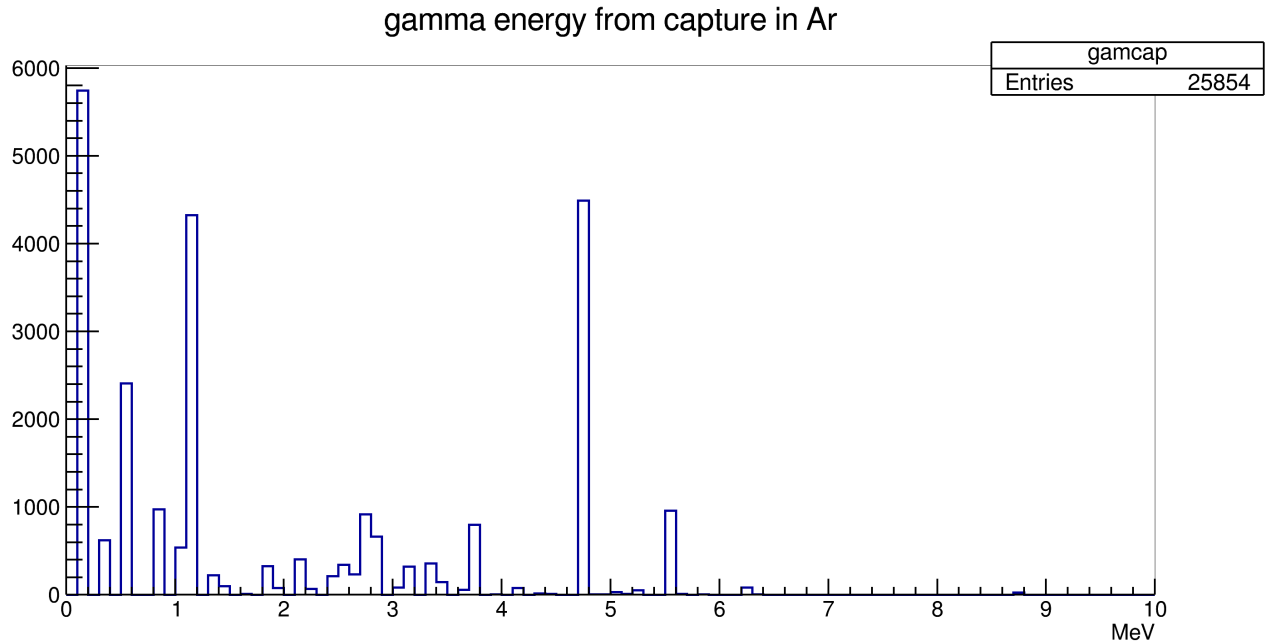


Figure 10: spectrum of gamma rays from neutron captures in the active LAr region

summed in a single cluster. No threshold is set on the minimum cluster energy. No noise nor charge attenuation nor charge recombination are considered.

Clusters are built only if the electron/positron is generated in the active LAr region.

In the tree, every particle carries track of the last neutron interaction in its history. Thus, different components in the cluster spectra can be isolated.

The result of this exercise is in figure 13. Again, three spectra are shown: clusters from capture in LAr, clusters from all types of interactions in LAr, clusters from neutron interactions in other materials. Here, no selection is made on the position of the neutron LAr interaction: both active and inactive regions are accepted, since the γ spectrum will be the same.

The double escape peak is visible in the LAr spectra, although experimental effects will clearly broaden it and make it more elusive. Another peak is visible and could be reconstructed, corresponding to the double escape peak from the 7.6 MeV γ from capture on Iron. Compton edges are also visible.

8 Conclusions

This standalone simulation of the Cold Box neutron generator setup allows to understand the major features of neutron propagation and interactions in it.

It appears that neutron thermalization is dominated by materials in the structure of the cold box and in the shielding of the neutron generator, rather than by argon.

In particular, hydrogenated materials affect heavily the capture rate, while structural materials affect the γ background.

A very naive exercise at particle level confirms the plausible presence of a signal due to double escape from the 4.7 MeV γ produced in neutron captures on ^{40}Ar .

No other external or internal background has been assumed here, these will be the subject of further simulations.

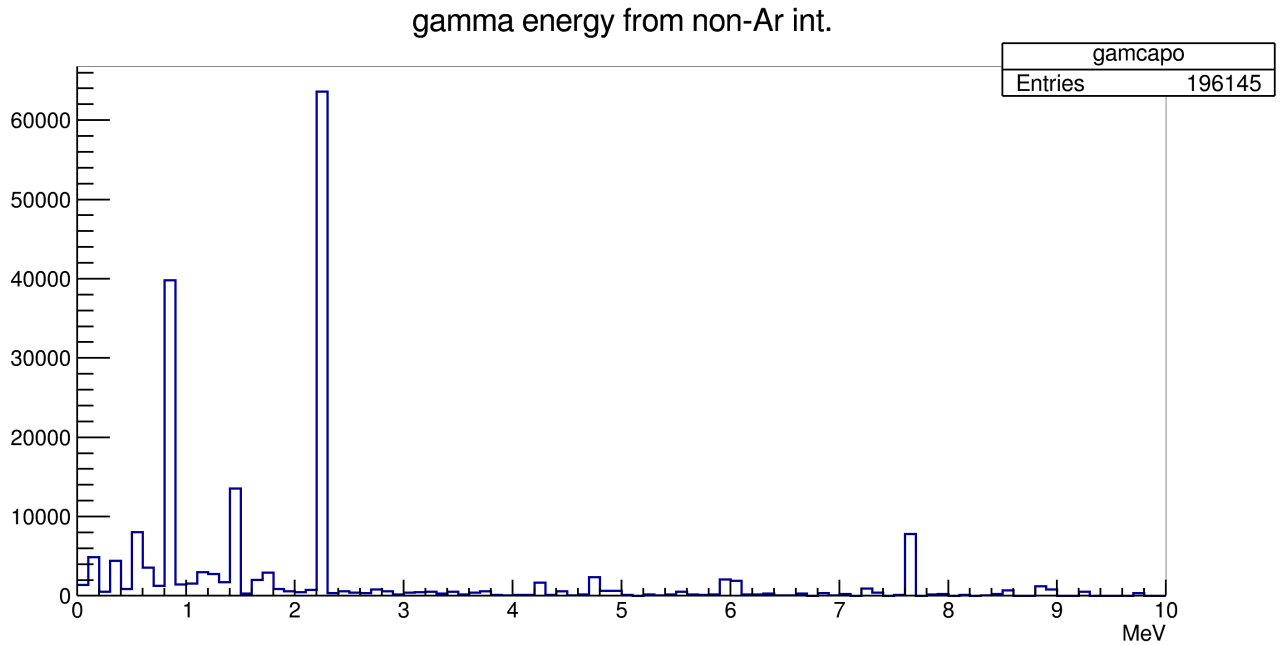


Figure 11: Spectrum of gamma rays from neutron interactions in materials different from LAr

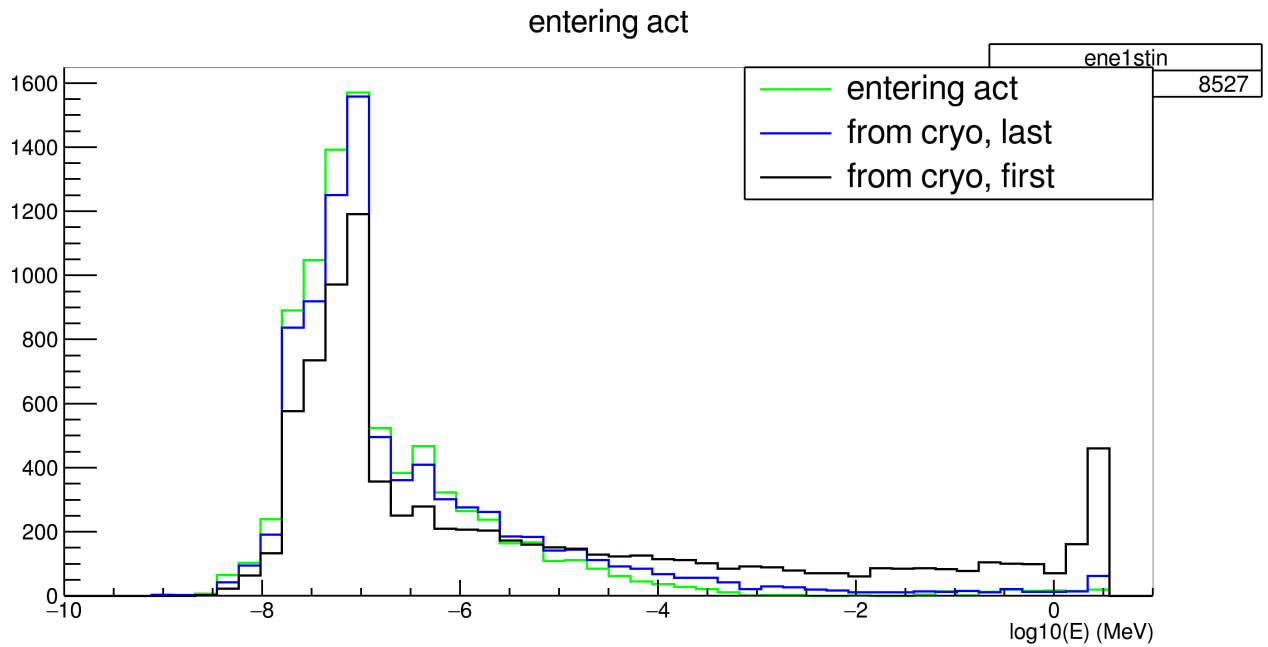


Figure 12: Events with a neutron capture in the active LAr: energy spectra of neutrons at the three stages described in the text

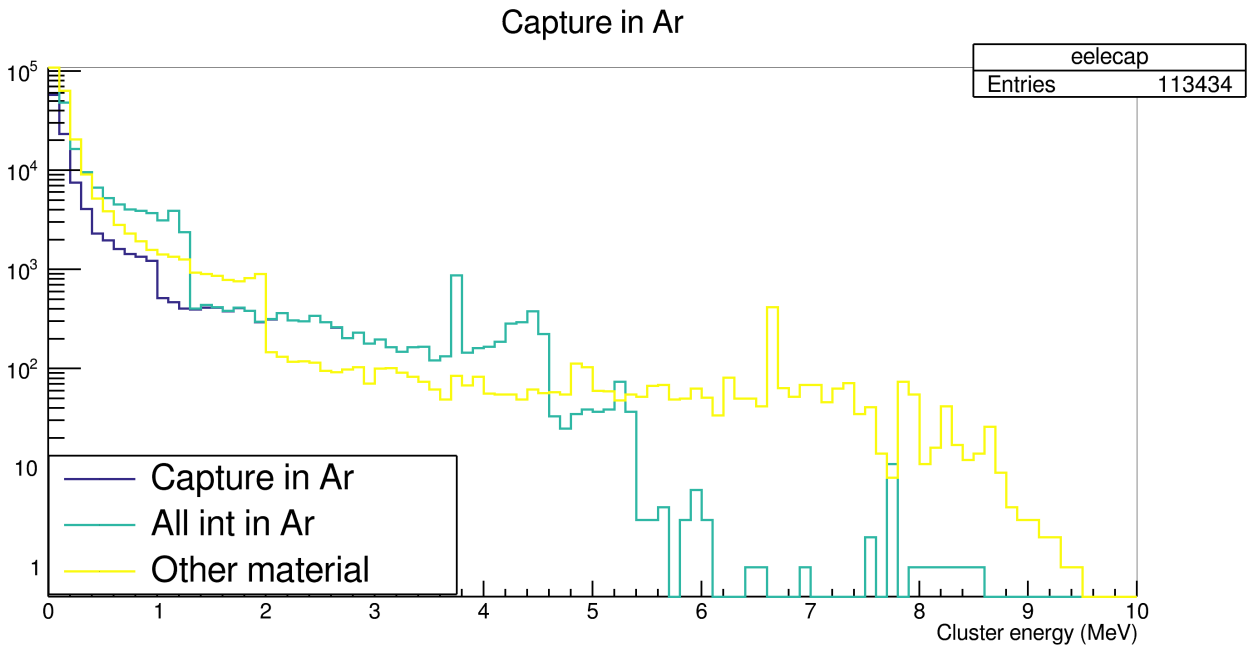


Figure 13: pseudo-clusters of deposited energy, obtained from particle-level information as described in the text.

A HeaderTree

The HeaderTree contains informations about the primary particle and the global energy deposition/ optical photons/ captures in each event

- Int_t RunNum; Run number
- Int_t EveNum; Event number
- Float_t Vertex[3]; Position where the primary particle was generated
- Int_t Primary; id of primary particle (PDG numbering)
- Float_t P_Primary[5]; 3-momentum, total energy, kinetic energy of primary
- Int_t ncaptures; number of captures in the LAr active volume
- Float_t Edepot; Energy deposited in the LAr active volume
- Float_t phetot; total number of optical photons reaching the photon detectors *divided by ten*

B HitsTree

HitsTree contains information about inelastic interactions, boundary crossings, energy depositions, optical photons. It has the same RunNum and EveNum as the HeaderTree to ensure event correspondence. We can divide it into blocks:

B.1 Boundary crossings

Variable dealing with boundary crossings or particles below threshold have the string “Inc” in their name

- Int_t NIncHits; Total number of “Inc” hits
- Int_t IdInc[MAXHITS]; Identity (PDG) of the particle
- Int_t TrInc[MAXHITS]; Track number of the particle
- Int_t IntParInc[MAXHITS]; Identity of the “parent” from last inelastic interaction
- Int_t RegInc[MAXHITS]; Region of the boundary crossing: if positive the particle is entering, if negative the particle is exiting. Region 13 is inactive LAr, region 14 is active LAr
- Float_t PosInc[MAXHITS][3]; position in space of hit
- Float_t PInc[MAXHITS][5]; 3 momentum, total energy, kinetic energy of crossing particle
- Float_t TimeInc[MAXHITS]; time **nanoseconds**

B.2 Inelastic Interactions

The inelastic int are in the variables with “Ine” in the name. For each Int, up to NIneHits, you have the information of the position, **region number** type, time, and particle type originating the interaction. You also have the number of generated secondaries. All secondaries in an event are stored in a list up to NIneSec. Cross-reference between interaction and secondary is provided by the index of hit attached to the secondary, and to the index of first secondary attached to the hit. For each particle, there is also the memory of the last neutron interaction from which the particle originates. For instance, in the list of secondaries there can be an electron produced in a Compton interaction by a photon that was produced in a neutron capture. Attached to the electron there is the code (306) of this neutron capture, the region where it occurred, and the index in the Ine hits list of this capture. For all particles, you also get a “track number”, this is incremented each time a new particle is generated, and attached to it.

- Int_t NIneHits; number of inelastic/decay interactions
- Int_t TypeIne[MAXINEHITS]; int. type (fluka coding, see below)

- Int_t IdIne[MAXINEHITS]; PDG identity of the incoming particle
- Int_t TrIne[MAXINEHITS]; track number
- Int_t IntParIne[MAXHITS]; parent from last interaction
- Float_t PIne[MAXINEHITS][5]; 3-momentum, total energy, kinetic energy of incoming particle
- Float_t PosIne[MAXINEHITS][3]; position of hit
- Float_t TimeIne[MAXINEHITS]; time
- Int_t NSecIne[MAXINEHITS]; number of secondaries in this hit
- Int_t FirstSec[MAXINEHITS]; index of first secondary from this hit in the list of secondaries
- Int_t RegIne ; region where the interaction occurred. A list of regions is in the appendix
- Int_t NTIneSec; total number of secondaries in this event
- Float_t PSec[MXS][5]; momentum,total energy,kinetic of secondary particle
- Int_t TrSecIne[MXS]; track number
- Int_t HitSecIne[MXS]; hit where particle was produced
- Int_t IdSecIne[MXS]; PDG identity of this secondary
- Int_t ASecIne[MXS]; A of secondary if ion
- Int_t ZSecIne[MXS]; Z of secondary if ion
- Int_t NeuOldSec[MXS]; Last neutron interaction type in this particle history
- Int_t NeuRegSec[MXS]; Region where the last neutron interaction occurred
- Int_t NeuOldVtx ; Index in the hit list (NIneHits) of the last neutron interaction

B.3 Energy deposition

- Int_t NCalHits; number of energy "blobs" in grid
- Int_t WhCal[MAXHITS]; not used
- Float_t PosCal[MAXHITS][3]; /position in space of n-th blob
- Float_t EneCal[MAXHITS]; energy deposited in blob

NCHitNCap,PosCNCap, EneCNCap : same as above counting only neutron captures in active LAr

B.4 Optical photons

Optical photons are collected in 4 tiles, numbered 0 to 3. Tile number 2 is the most active. A "hit" here is identified by the tile number, and the arrival time of optical photons. Arrival times are quantized in bins of 16 nanoseconds.

- Int_t NPheHits ; number of hits in tiles
- Float_t Phe[MAXHITS]; number of optical photons in this hit of hit
- Int_t PheTile[MAXHITS]; which tile of hit
- Float_t PheTime[MAXHITS]; time of hit
- Float_t TotPhe[4]; total optical photons in each tile, integrated over time

NPheHitsNCap, PheNCap, PheTileNCap, PheTimeNCap[MAXHITS] TotPheNCap[4] same as above counting only neutron captures in active LAr

C reaction codes

```
* Icode = 99: call from Doiosp, ion splitting secondaries *
* Icode = 1xy: call from Kaskad (hadrons, muons *
* 100: elastic interaction secondaries *
* 101: inelastic interaction secondaries *
* 102: particle decay secondaries *
* 103: delta ray generation secondaries *
* 104: pair production secondaries *
* 105: bremsstrahlung secondaries *
* 106: de-excitation in flight secondaries *
* 110: radioactive decay products *
* Icode = 2xy: call from Emfsco (electro-magnetic *
* 208: bremsstrahlung secondaries *
* 210: Moller secondaries *
* 212: Bhabha secondaries *
* 214: in-flight annihilation secondaries *
* 215: annihilation at rest secondaries *
* 217: pair production secondaries *
* 219: Compton scattering secondaries *
* 221: photoelectric secondaries *
* 225: Rayleigh scattering secondaries *
* 230: inverse Compton secondaries *
* 237: mu pair production secondaries *
* Icode = 30x: call from Kasneu - low energy neutrons *
* many: interesting ones are *
* 302: elastic *
* 303: generic inelastic (some specific channels below) *
* 304: n,2n *
* 305: n,fission *
* 306: n capture *
* 307: n,n'gamma on first excited state *
* 364: n,p *
```

D Region numbers, names, and materials

1	BLKBODY	BLCKHOLE	External limit
2	VOID	VACUUM	Void around the geometry
3	Cryfoam	FOAM	Cryostat foam
4	CrySSinc	COLDSS	Cryostat steel internal, cold
5	CrySSinh	WARMSS	Cryostat steel internal, warm
6	CrySSou	WARMSS	Cryostat steel external
7	Airout	AIR	Air
8	ShieldPb	LEAD	Lead in the neutron generator shielding
9	ShieldPo	Polystyr	Plastic in the neutron generator shielding
10	Shieldv	PolyBor	Borated poly in the neutron generator shielding
11	Shole	AIR	cavities in the neutron generator shielding
12	LArGas	ARGGAS	gaseous Ar
13	LArIna	ARGON87B	LAr not readout, both below and above anodes
14	LArAct	ARGON87	LAr readout
15	Anode1	G10	Anode
16	Anode2	G10	Anode
17	AnEpox	EGlassr	Anode support
18	AnSS	SSbars	Anode frame
19	AnLAr	ARGON87B	LAr around anodes
20	PDSfram	G10	Frame around the PDS

21	PDS0	POLYETHY	PDS
22	PDS1	POLYETHY	
23	PDS2	POLYETHY	
24	PDS3	POLYETHY	
25	PDSLAr	ARGON87B	LAr in between the PDS
26	DDtube	WARMSS	Neutron generator tube